21%-EFFICIENT SILICON SOLAR CELLS USING AMORPHOUS SILICON REAR SIDE PASSIVATION

Marc Hofmann, Stefan Glunz, Ralf Preu and Gerhard Willeke
Fraunhofer Institute for Solar Energy Systems (ISE)
Heidenhofstrasse 2, D-79110 Freiburg, Germany
phone: +49 761-4588-5614; fax: +49 761-4588-9250
email: marc.hofmann@ise.fraunhofer.de

ABSTRACT: Stacks of amorphous silicon and silicon oxide – all deposited by PECVD – are used to passivate the rear surfaces of high-efficiency solar cell structures on p-type float zone substrates. Energy conversion efficiencies of up to 21.7 % can be reported. An investigation of the effect of a post-process annealing at different temperatures is presented with I-V and IQE measurements leading to the conclusion that the rear surface passivation is stable until a temperature of 400 °C. Additionally, investigations on the passivation quality of single layer amorphous silicon and stacks of amorphous silicon and silicon oxide were performed. Surface recombination velocities below 6 cm/s could be measured leading to an excellent surface passivation of p-type float zone wafers (1 Ω cm).
Keywords: a-Si, High-Efficiency, PECVD

1 INTRODUCTION

One of the key technologies for the increase of silicon wafer solar cell efficiency and the decrease in cost per peak power is the passivated and locally contacted rear surface. The well-known PERC (passivated emitter and rear cell) concept [1] is the role model for a high-efficiency rear side. Using Fraunhofer ISE's laser-fired contacting technology (Laser-Fired Contacts, LFC) this high-efficiency rear side can be fabricated in a cost-effective and convenient way [2]. The LFC technology is patented [3].

2 PASSIVATION LAYERS

The passivation of the crystalline silicon solar cell's rear surface with suited layer systems is one of the main research topics at the moment.
Thermally grown silicon dioxide layers are well-developed and used as a standard material in semiconductor technology. However, the fabrication of these layers does not perfectly fit in the solar cell production process due to the needed high temperatures (~1000 °C) and its relatively long process time. Oliver Schultz et al. have shown that a rear surface passivation using thermally grown oxide layers produced in a wet process at around 800 °C can lead to record-breaking multicrystalline silicon solar cells [4]. Also stacks of thin thermal wet oxide and plasma-enhanced chemical vapour deposited (PECVD) silicon oxide (SiO_x) are successfully used by the same group [5].
However, a rear surface passivation process that is quicker and at lower process temperatures leading to the same or better results would be preferable.
A quite extensively studied candidate for the rear surface passivation is PECVD silicon nitride (SiN_x). Different research groups have found that SiN_x layers can lead to very low surface recombination velocities [6],[7],[8]. This passivation effect seems at least partly to be due to the field effect passivation of fixed positive charges in the SiN_x layer which influence the ratio of electrons and holes at the p-type silicon surface. This can lead to an inversion layer on the surface of the bulk p-type Si material [9]. If local contacts are applied to the solar cell's rear surface a contact to both the inversion (n-type) layer and the bulk p-type silicon is formed and leads to a parasitic shunting and a decrease in efficiency.
We have introduced stack layers of SiN_x and SiO_x – both deposited by PECVD – in order to improve thermal stability and internal reflection in 2004 [10].
A promising alternative is the use of hydrogenated amorphous silicon (a-Si:H, in short a-Si) layers which also can be deposited via PECVD.

3 HYDROGENATED AMORPHOUS SILICON

a-Si layers have been investigated by different research groups in order to provide an efficient surface passivation on p-type silicon wafers [11],[12],[8]. Indeed, excellent surface passivation results could be reported. Also very good solar cell performances of up to 20.5 % efficiency have been achieved using a-Si as a rear surface passivation layer and laser-fired rear contacts [13]. Even higher efficiencies have been reached for rear surface structures with a stack system of undoped and doped a-Si, µc-Si and ZnO:Al (without local contacts). Independently confirmed 21.0 % efficiency [14] and non-confirmed 21.4 % (P. J. Rostan et al. at Silicon Forest Workshop 2006, unpublished) for this stack system have been reported. Sanyo's HIT structure with its outstanding 21.8 % efficient cell uses a special amorphous-crystalline heterojunction cell concept with intrinsic amorphous silicon passivating both surfaces of the crystalline silicon substrate [15].

4 LIFETIME INVESTIGATION

4.1 Experimental

Investigations on PECV-deposited a-Si as a passivation layer for p-type silicon wafer surfaces have been performed at Fraunhofer ISE. The substrates used were 1 Ω cm boron-doped p-type float zone (FZ) wafers with a thickness of 250 µm and shiny-etched surfaces.
Prior to the deposition the wafers were cleaned in a standard wet chemical bath sequence (RCA clean, including a final dip in fluoric acid (HF)).
Depositions took place in a direct plasma reactor with an excitation frequency of 13.56 MHz using a gas mixture of silane (SiH_4) and hydrogen (H_2).
Both surfaces of the substrates were coated in order to manufacture a symmetrical sample structure (see Fig. 1) which makes it easy to extract the surface recombination velocity from carrier lifetime measurements. The

measurement of the lifetimes took place using a WCT-100 machine by Sinton Consulting [16].

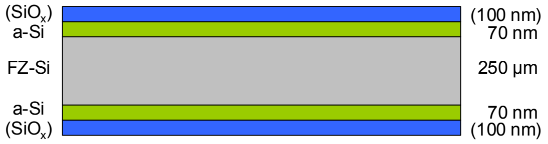

Fig. 1: Sketch of the sample structure for the lifetime investigation. Samples with and without an additional SiO_x layer were fabricated.

The maximum surface recombination velocity has been calculated under the estimation that no Shockley-Read-Hall recombination in the bulk takes place. Then, the bulk lifetime of the silicon wafer is mainly limited by Auger recombination. The calculation of the bulk lifetime was done by use of the Auger recombination model of Glunz and Rein [17]. Using its result, the surface recombination velocity can be calculated by the following equation [18]:

$$\frac{1}{\tau_{eff}} = \frac{1}{\tau_b} + \left(\frac{W}{2S_{eff}} + \frac{1}{D_n}\left(\frac{W}{\pi}\right)^2 \right)^{-1} \qquad \text{Equation (1)}$$

with the silicon wafer's bulk lifetime τ_b, the wafer's thickness W, the effective surface recombination velocity S_{eff} and the diffusion constant for electrons D_n.

For the upcoming implementation of the passivation layer in a solar cell structure an investigation of the dependence of the passivation quality on the presence of an additional PECVD silicon oxide (SiO_x) layer on top of the a-Si layer was performed.

4.2 Results

After an optimisation of the deposition parameters lifetimes of more than 1 ms could be measured. In Fig. 2 the results of the lifetime measurement can be seen.

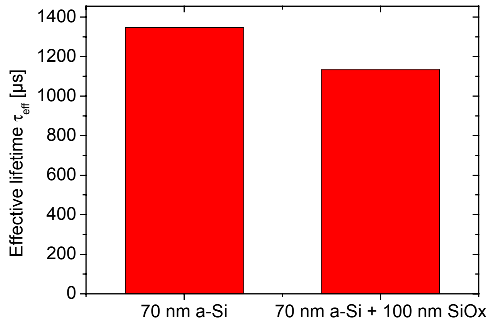

Fig. 2: Effective lifetime at $\Delta n = 5 \cdot 10^{14}$ cm^{-3} of a-Si passivated FZ wafers (250 µm thickness, p-type, boron doped, 1 Ω cm, shiny etched surfaces).

Using equation 1, the lifetime values could be transformed to maximum surface recombination velocities (see Fig. 3) of 4 cm/s to 6 cm/s.

These results show the potential of a-Si layers as a means for excellent surface passivation.

Additionally, it is expected that the passivation effect is mainly due to minimising the density of interface traps D_{it}. Therefore, a shunting effect as with SiN layers is not anticipated.

5 SOLAR CELLS

To show the capability of a-Si layers as a rear surface passivation layer high-efficiency solar cells were fabricated.

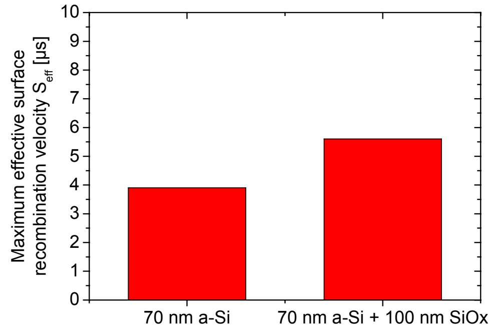

Fig. 3: Maximum effective surface recombination velocities of a-Si passivated FZ wafers (250 µm thickness, p-type, boron doped, 1 Ω cm, shiny etched surfaces).

5.1 Experimental

These solar cells were made of 0.5 Ω cm boron-doped p-type float zone (FZ) wafers with a thickness of 250 µm and shiny-etched surfaces. So, almost the same type of wafers as in the lifetime experiment except the increased doping concentration is used.

The solar cells' structure can be found in Fig. 4.

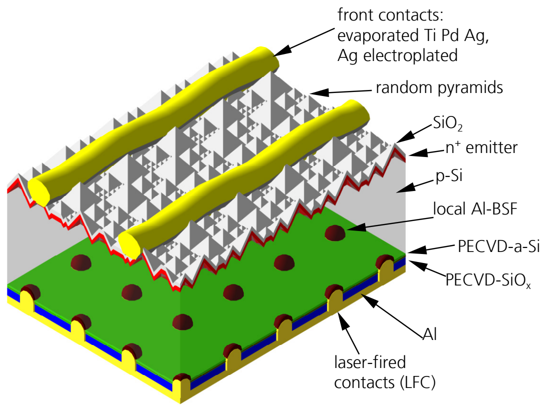

Fig. 4: Scheme of the fabricated solar cells.

The cells exhibit evaporated TiPdAg front contacts, a thermally oxidised anti-reflection coating that also serves as front passivation layer, an 120 Ω/sq n-type emitter, a 0.5 Ω cm p-type bulk, PECVD-a-Si and -SiOx, an evaporated Al layer at the back and laser-fired contacts that led to a local Al-BSF underneath (above if looking at Fig. 4) the point contacts.

The a-Si (~70 nm) and SiO_x (~100 nm) layers used are the same as were investigated in the lifetime experiment.

After finishing the cells, the I-V characteristics were measured. Subsequently, the cells were annealed at different temperatures in forming gas for 15 min (excluding 10 min of ramping up the temperature) to find the optimum annealing temperature for front and rear passivation and for the local laser-fired rear contacts. The challenge was to find a temperature that would increase the front passivation and the rear contacts without harming the rear passivation.

Then, the I-V-characteristics of the cells were measured again.

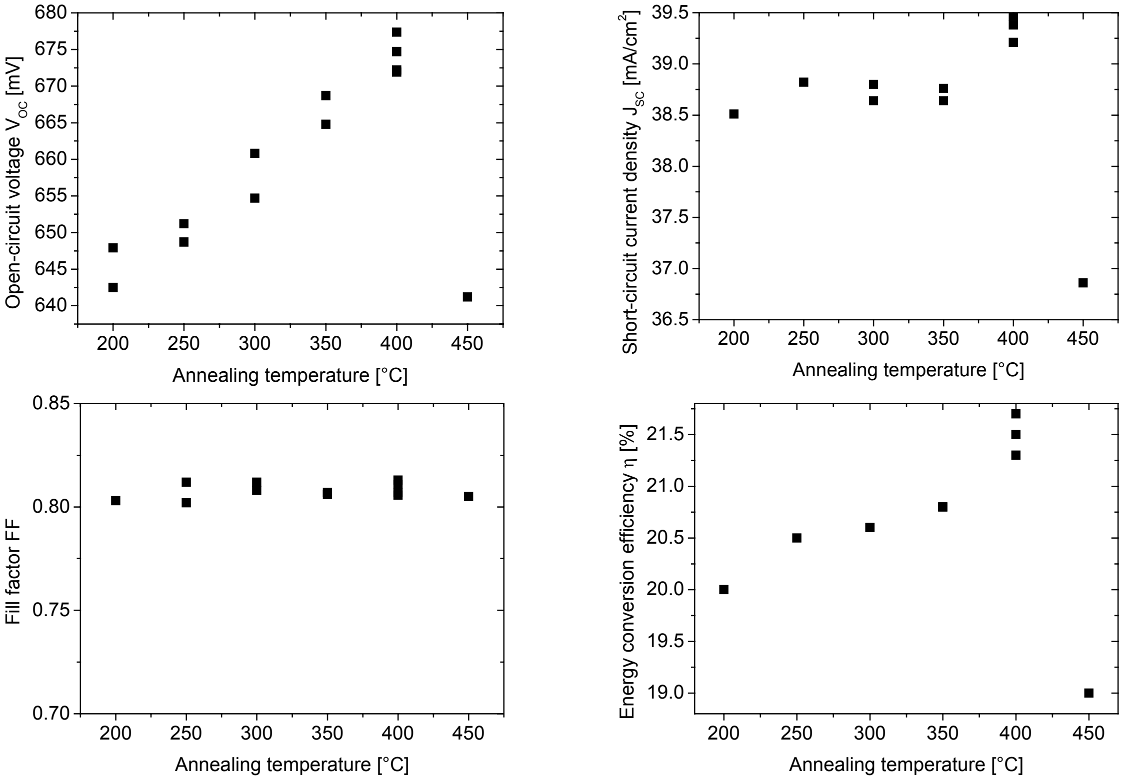

Fig. 5: I-V characteristics of the manufactured cells in dependence on the temperature of a post-process annealing step.

5.2 Results

The solar cell parameters showed a strong dependence on the annealing temperature as can be seen in Fig. 5.The open-circuit voltage V_{oc} is steadily increasing with annealing temperature from 200 °C to 400 °C, from around 645 mV to around 676 mV. At 450 °C the voltage decreases strongly to about 642 mV.

Almost the same behaviour could be found for the short-circuit current J_{sc}. It rises from 38.5 mA/cm^2 (200 °C) to 39.3 mA/cm^2 (400 °C). Also at 450 °C J_{sc} decreases to a value below 37 mA/cm^2.

For the fill factor FF it can be stated that the contacting processes were very successful leading to values above 80 % for all cells.

The energy conversion efficiency η is calculated from the three mentioned parameters. Therefore, it is clear now that also the efficiency is steadily increasing for annealing temperatures from 200 °C to 400 °C with values of 20.0 % to 21.7 %. The strong decrease at 450 °C can be found as well (19.0 %).

The best achieved energy conversion efficiency of 21.7 % has been confirmed by the Fraunhofer ISE CalLab. The cell's exact measured parameters can be found in Table I.

Table I: Measured parameters of the best solar cell of this investigation. Independently confirmed by Fraunhofer ISE CalLab.

Area	V_{oc}	J_{sc}	FF	η
4.0 cm^2	677 mV	39.5 mA/cm^2	81.1 %	21.7 %

The question that arises clearly is, which physical effect drives the efficiency to these values. To give insight into this question internal quantum efficiency (IQE) measurements were done at Fraunhofer ISE. Investigated samples were of the structure shown in Fig. 4 and annealed at temperatures between 200 °C and 450 °C in steps of 50 °C. Fig. 6 shows the results of the measurement.

In the short wavelength regime in the range of 300 nm to around 550 nm the effect of the solar cell's front surface can be found. The observed increase of quantum efficiency with higher annealing temperatures to about the same results at temperatures of 400 °C and 450°C is attributed to the annealing of the front surface passivation which is done by thermal oxidation. Therefore, the well-known oxide annealing effect has been observed. The quality of the solar cell's bulk and rear surface can be derived from the IQE at long wavelengths around 900 nm to 1200 nm. Here, very high values can be found. Hence, the quality of the bulk and the rear surface seems very satisfactory. For annealing temperatures of 200 °C to 400 °C the passivation properties of the rear surface is almost stable. Only a slight improvement with higher temperatures might be observable. When the temperature is increased further to 450 °C the performance of the solar cell's back deteriorates compared to the lower temperatures. This effect fits in the observation of an overall decreased cell performance of the 450 °C annealed cells at the I-V measuments. We attribute this effect to the de-passivation of the solar cell's back. Hydrogenated amorphous silicon is known for its quite low thermal stability. The observed de-passivation probably is due to the cracking of hydrogen bonds at the c-Si a-Si interface which are subjected to be important for the passivation effect. This leaves silicon dangling bonds and therefore Shockley-Read-Hall (SRH) active recombination centres at the interface.

The good news is that our passivation stack system of amorphous silicon and silicon oxide - all fabricated with

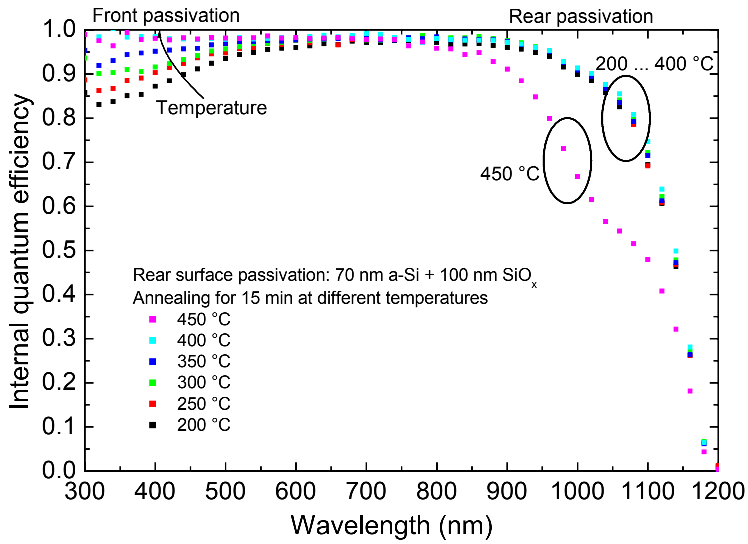

Fig. 6: Internal quantum efficiency of solar cells annealed at different temperatures vs. the wavelength of light. An increase in front passivation (thermally grown SiO_2) at short wavelengths with annealing temperature could be found. The rear passivation (a-Si + SiOx) is stable until 400 °C but decreases strongly at 450°C.

PECVD processes – could withstand the relatively long annealing step at 400 °C which lead to an outstanding cell performance.

6 SUMMARY

Stacks of amorphous silicon and silicon oxide – both deposited using a PECVD system – are successfully used for passivating crystalline silicon wafers, leading to surface recombination velocities below 6 cm/s. These stacks were used to passivate crystalline silicon solar cells' rear surfaces. This led to a maximum cell efficiency of 21.7 % on p-type (Boron doped) float zone silicon substrates with a thickness of 250 µm. The cells' area was 4.0 cm^2. I-V and IQE measurements lead to the conclusion that the front surface passivation (thermally grown SiO_2) increased with annealing temperature and the rear surface passivation (a-Si + SiO_x) was stable until 400 °C.

7 OUTLOOK

The deposition of amorphous silicon layers using a large area PECVD reactor already led to excellent results which will be published elsewhere.

ACKNOWLEDGEMENTS

The authors would like to thank A. Leimenstoll, S. Wassie and S. Seitz for clean room processing. Additionally, the authors thank E. Schäffer for I-V and IQE measurements and B. Hund for the measurements in the Fraunhofer ISE CalLab.
This work was partly supported by the EU funded project „Crystal Clear" under the project number SES6-CT2003-502583.

REFERENCES

[1] A. W. Blakers, J. Zhao, A. Wang et al., Proceedings of the 9th European Photovoltaic Solar Energy Conference, Freiburg, Germany (1989) 328.
[2] E. Schneiderlöchner, R. Preu, R. Lüdemann et al., Progr. Photovolt. 10 (2002) 29.
[3] R. Preu, E. Schneiderlöchner, S. Glunz et al., No. WO002002025742A3 (2001).
[4] O. Schultz, S. W. Glunz, and G. Willeke, Progr. Photovolt. 12 (2004) 553.
[5] O. Schultz, M. Hofmann, S. W. Glunz et al., Proceedings of the 31st IEEE Photovoltaic Specialists Conference, Orlando, Florida, USA (2005) in press.
[6] H. Mäckel and R. Lüdemann, J. Appl. Phys. 92 (2002) 2602.
[7] B. Lenkeit, Dissertation Thesis, Universität Hannover, 2002.
[8] S. de Wolf, Dissertation Thesis, Katholische Universität Leuven, 2005.
[9] S. Dauwe, L. Mittelstädt, A. Metz et al., Progr. Photovolt. 10 (2002) 271.
[10] M. Hofmann, E. Schneiderlöchner, W. Wolke et al., Proceedings of the 19th European Photovoltaic Solar Energy Conference, Paris, France (2004) 1037.
[11] S. Dauwe, Dissertation Thesis, Universität Hannover, 2004.
[12] M. Schaper, J. Schmidt, H. Plaqwitz et al., Progr. Photovolt. 13 (2005) 381.
[13] W. Brendle, V. X. Nguyen, A. Grohe et al., Progr. Photovolt. (2006) in press.
[14] P. J. Rostan, U. Rau, V. X. Nguyen et al., Sol. Ener. Mater. Sol. Cells 90 (2006) 1345.
[15] E. Maruyama, A. Terakawa, M. Taguchi et al., Proceedings of the 4th World Conference on Photovoltaic Energy Conversion, Waikoloa, Hawaii, USA (2006) in print.
[16] R. A. Sinton, A. Cuevas, and M. Stuckings, Proceedings of the 25th IEEE Photovoltaic Specialists Conference, Washington DC, USA (1996) 457.
[17] S. W. Glunz, D. Biro, S. Rein et al., J. Appl. Phys. 86 (1999) 683.
[18] A. B. Sproul, J. Appl. Phys. 76 (1994) 2851.